The EMBO Journal vol.15 no.18 pp.4844–4851, 1996

Native structure and arrangement of inositol-1,4,5-trisphosphate receptor molecules in bovine cerebellar Purkinje cells as studied by quick-freeze deep-etch electron microscopy

Eisaku Katayama[1], Hisayuki Funahashi, Takayuki Michikawa[2], Tomoko Shiraishi, Takaaki Ikemoto[3,4], Masamitsu Iino[3], Kazushige Hirosawa and Katsuhiko Mikoshiba[2]

Departments of Fine Morphology and [2]Molecular Neurobiology, Institute of Medical Science, The University of Tokyo, Minato-ku Tokyo 108 and [3]Department of Pharmacology, Faculty of Medicine, University of Tokyo, Bunkyo-ku, Tokyo 113, Japan

[4]Present address: Department of Pharmacology, Saitama Medical School, Moroyama-cho, Saitama 350-04, Japan

[1]Corresponding author

We used quick-freeze deep-etch replica electron microscopy to visualize the native structure of inositol-1,4,5-trisphosphate receptor (IP_3R) in the cell. In the dendrites of Purkinje neurons of bovine cerebellum there were many vesicular organelles whose surfaces were covered with a two-dimensional crystalline array of molecules. Detailed examination of the cytoplasmic true surface of such vesicles in replica revealed that the structural unit, identified as IP_3R by immunocytochemistry and subsequent Fourier analysis, is a square-shaped assembly and is aligned so that the side of the square is inclined by ~20° from the row-line of the lattice. Comparison with the ryanodine receptor (RyaR), another intracellular Ca^{2+} channel on the endoplasmic reticulum, suggested that IP_3R, unlike RyaR, has a very compact structure, potentially reflecting the crucial difference in the function of the cytoplasmic portion of the molecule.

Keywords: cerebellar Purkinje neuron/inositol-1,4,5-trisphosphate receptor/*in situ* structure/quick-freeze deep-etch electron microscopy/ryanodine receptor

Introduction

Among various receptor proteins involved in intracellular signal transduction, the inositol-1,4,5-trisphosphate receptor (IP_3R) and the skeletal-type ryanodine receptor (sRyaR) are unique in that they form Ca^{2+} channels by themselves on the endoplasmic reticulum (Ferris *et al.*, 1989; Maeda *et al.*, 1991a; Hirota *et al.*, 1995; see also the reviews by Mikoshiba *et al.*, 1994; Furuichi *et al.*, 1994; Pozzan *et al.*, 1994). Complementary DNAs for both receptors were cloned and their nucleotide sequences were determined (Furuichi *et al.*, 1989; Takeshima *et al.*, 1989; Mignery *et al.*, 1990). The primary amino acid sequences deduced from such data show a certain degree of homology, suggesting a similarity not only in structure but also in some aspects of function of these proteins expressed inside the cell. Both receptors share the sequences corresponding to a putative membrane-spanning region close to the carboxy-terminal end, and the major amino-terminal portion facing the cytoplasm to receive the signals. The membrane-spanning moieties are highly homologous, probably contributing to the common tetrameric nature of the receptors. However, the homology in the amino-terminal segment is limited, and there may be some crucial difference in its functions. For instance, IP_3R is involved in IP_3-induced Ca^{2+} release whereas sRyaR, coupled with (dihydropyridine-sensitive) L-type Ca^{2+} channels, is believed to be involved in a Ca^{2+}-induced Ca^{2+} release mechanism. It is reasonable to expect that such functional differences may potentially be reflected in the basic architecture of the receptor molecules.

sRyaR was identified as the so-called 'foot' structure which had been discovered as a highly differentiated apparatus connecting the transverse tubule and junctional sarcoplasmic reticulum (SR) of striated muscle (Franzini-Armstrong, 1970; Franzini-Armstrong and Nunzi, 1983). Electron microscopy of detergent-solubilized and purified sRyaR molecules showed its characteristic four-leaf-clover shape whose surface profiles look similar to the structure of the 'foot' as observed *in situ* in muscle cells using the freeze-fracture technique (Block *et al.*, 1988; Saito *et al.*, 1988). Further, three-dimensional reconstruction from the images obtained either by negative staining (Wagenknecht *et al.*, 1989) or by cryo-electron microscopy (Radermacher *et al.*, 1994) revealed a substructure indicating the presence of an intramolecular passage or cavity which may possibly act as the Ca^{2+} channel.

One of the richest sources of IP_3R is the Purkinje neuron in vertebrate cerebellum (see reviews by Mikoshiba *et al.*, 1994; Furuichi *et al.*, 1994; Pozzan *et al.*, 1994). There, IP_3R and sRyaR have been shown to co-exist in smooth-surfaced endoplasmic reticulum (sER) (Walton *et al.*, 1991), which sometimes forms a very prominent array of membranous cisternae called 'cisternal stacks' (Herndon, 1964; Karlsson and Scultz, 1966; Van Nimvegen and Sheldon, 1966; Hansson, 1981; Yamamoto *et al.*, 1991; Takei *et al.*, 1994). All of the cytoplasmic space between such cisternae is filled with numerous electron-dense particles forming intermembranous bridges (Otsu *et al.*, 1990; Yamamoto *et al.*, 1991) which, in some areas, look regularly spaced just like the appearance of the foot structure on the junctional SR of muscle. In contrast to the sRyaR molecule whose higher order structure remained stable in detergent, IP_3R isolated in a similar manner was not suitable material for electron microscopic studies of its organized molecular architecture. Though the negatively stained image of the IP_3R which was solubilized by detergent and purified from cerebellum (Maeda *et al.*, 1991b) or smooth muscle (Chadwick *et al.*, 1990) contained some particles suggesting its tetrameric structure, both the size and the overall shape appeared quite variable, and it was hard to deduce its native structure *in situ*.

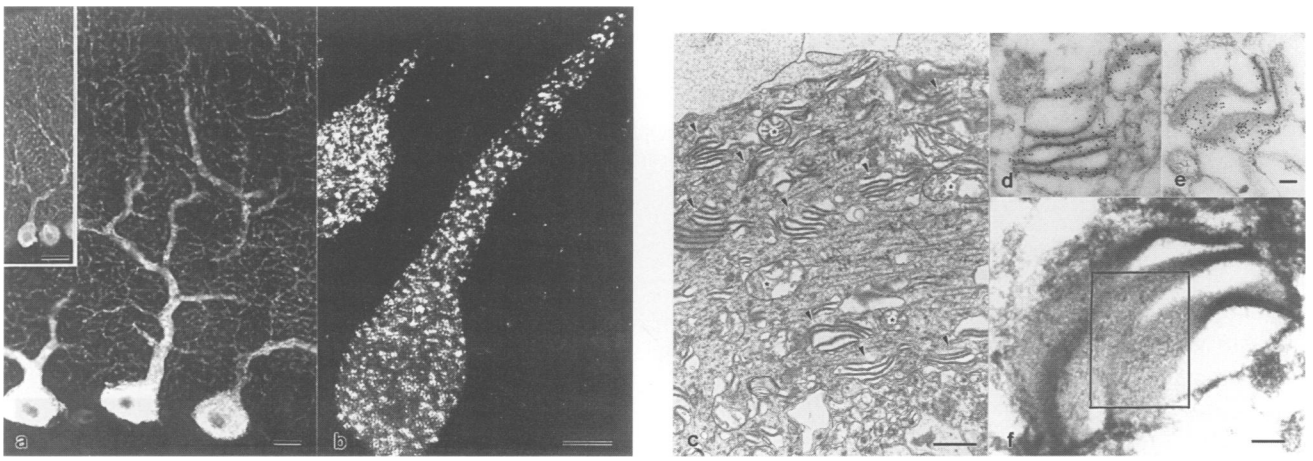

Fig. 1. (**a**) Immunofluorescence image of Purkinje neurons in bovine cerebellum. Conventional cryosections were stained with anti-IP_3R antibody. Note the very large size of the bovine Purkinje cell as compared with that of mouse (inset) at the same magnification. Scale bars represent 20 μm. (**b**) Semi-thin section from quick-frozen, freeze-substituted and plastic-embedded bovine cerebellum stained with anti-IP_3R antibody followed by fluorescent secondary antibody. The image was taken with a cooled-CCD camera (SBIG ST-8; 1536×1032 pixels, 14-bit dynamic range). Purkinje neurons are exclusively stained. Numerous dots are present both in the cell body and the dendrite. Some of them are apparently clustered. Scale bar indicates 10 μm. (**c**) Electron micrograph of a longitudinal section of a Purkinje cell dendrite. The cytoplasm contains two kinds of definable membranous structures; mitochondria (small asterisk) and sER in the form of 'cisternal stacks' (arrowhead). Scale bar indicates 0.5 μm. (**d**) and (**e**) Micrographs indicating immunocolloidal gold staining of cisternal stacks with anti-IP_3R antibody. In (d), colloidal gold particles distribute on the external surface of organelles and in the cytoplasmic space between stacks; (e) includes a portion cut parallel to the plane of the membrane stacks, which also is stained with anti-IP_3R antibody. (**f**) The field containing cisternal stacks similar to (e). The area defined by the rectangular border was digitized and subjected to Fourier transformation as shown in Figure 2. Scale bars correspond to 0.1 μm for (d–f).

Quick-freeze deep-etch replica electron microscopy as developed by Heuser (1979) is a unique technique which can provide clear and useful images of purified molecules adsorbed on mica flakes (Heuser, 1983, 1989; Katayama, 1989) or those existing inside live cells or tissues (Heuser, 1981; Katayama *et al.*, 1996). The three-dimensional structure of a model protein molecule (F-actin) adsorbed on a mica surface was excellently preserved by this technique, with unanticipated high spatial resolution (Morris *et al.*, 1994; Katayama *et al.*, 1996). Since the molecules on the membrane surface *in situ* should have an analogous topography to those on mica, one might expect the images of such particles to be similar in quality to those on mica. Hence, we attempted to visualize the structure of the unperturbed IP_3R molecules organized in the native intracellular environment.

We used bovine Purkinje cells as the material for freeze-fracture deep-etch visualization and found numerous vesicles in the dendrites whose surface is covered with a regular two-dimensional array of molecules. Combined use of immunocytochemistry and Fourier analysis enabled us to identify the structural element of this array as IP_3R molecules. Our present report is the first demonstration of the native structure and the mode of existence of IP_3R molecules, i.e as a Ca^{2+} channel on the endoplasmic reticulum, in the cerebellar Purkinje cell.

Results

Distribution of inositol 1,4,5-trisphosphate receptor molecules in bovine cerebellum

Figure 1a shows a row of Purkinje cells in a conventional frozen section of bovine cerebellum which was fluorescently stained by a specific antibody against IP_3R. The label was distributed as small distinct dots, which were especially evident in the dendritic portion of the cell. Figure 1b shows an enlarged view of the fluorescently stained semi-thin section from a quick-frozen plastic-embedded sample of the cerebellum, which was prepared originally for electron microscopy. From these images, it becomes apparent that individual fluorecent dots are often clustered and correspond to structures existing inside the dendrite or the cell body of the Purkinje cells. We examined a similar specimen by electron microscopy to define the structure responsible for the stained dots (Figure 1c). Apart from mitochondria, the dendrites contained one organelle whose morphology would appear as small dots by immunofluorescence microscopy, a membranous structure with distinct stacks of lamellar vesicles: the so-called 'cisternal stacks' (Herndon, 1964; Karlsson and Scultz, 1966; Hansson, 1981; Takei *et al.*, 1994). Immunogold staining of quick-frozen and freeze-substituted samples unambiguously confirmed the accumulation of abundant IP_3R molecules, not only in between the stacks but also on the surface of the organelles (Figure 1d and e: see also Figure 4 of Takei *et al.*, 1992). According to semi-quantitative morphometric analyses by Rusakov *et al.* (1993), the distribution of the lateral distances between the intercisternal bridges might not be random but showed certain modes, suggesting a hint of some regular structure. The strategy we employed to analyse the potential order further was Fourier transformation, which is often used as a first choice under such circumstances. The image of cisternal stacks observed in a freeze-substituted and plastic-embedded section parallel to the membrane plane (Figure 1f), was digitized (Figure 2a) and subjected to Fourier transform by a computer. The spectrum (Figure 2b) showed a pair of symmetrical and prominent spots corresponding to ~16 nm spacing, together with somewhat weaker spots at ~19 nm spacing in a direction slightly away from perpendicular to the former. (The reason for the large difference in the intensity of the two sets of reflections is described in the legend of Figure 2b, and will become clear in the following sections.) Fourier

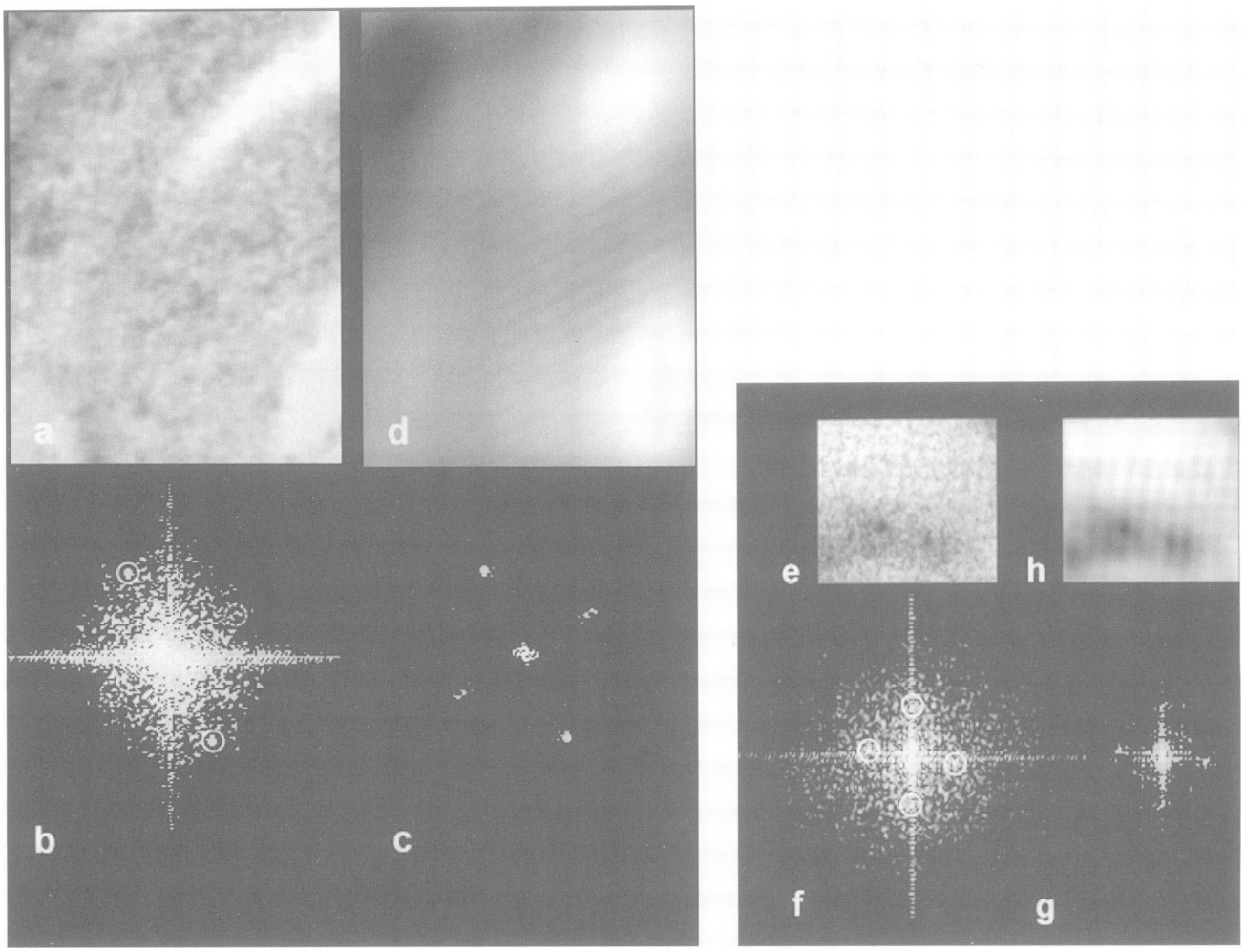

Fig. 2. (**a**) The same field as in Figure 1f after digitization. (**b**) Fourier spectrum of (a). The most prominent reflection spots are shown encircled, at a spacing of ~16 nm and the next are shown with dotted circles at ~ 19 nm. The sectioned specimen would include two adjacent membrane leaflets of cisternal stacks, giving rise to overlapping of two kinds of molecular arrays; one of which is the mirror image of the other. The stronger intensity of the first set of spots might be explained, at least partly, by the registered arrangement of the array to that direction, while the second set could split into weaker ones, since the lattice is not rectangular. (**c**) Selected spots used for reverse transform. These reflections were back-transformed to give the filtered image shown in (**d**). (**e**) The electron micrograph taken from the inset of Figure 5 of Takei *et al.* (1994) which was scanned and digitized for Fourier analysis. (**f**) Fourier spectrum of (e), whose most prominent peaks were extracted (**g**), and back-transformed to give the filtered image (**h**). The side length of the unit cell is 16.4 nm according to the authors' description. However, the actual ratio of spacing along two directions is ~7:8 and not 1:1, as indicated here. It should also be noted that the two lines connecting each pair of reflection spots in (g) do not cross with a right angle but are inclined by ~10°.

filtering, carried out by reverse transformation after masking the spectrum to pass the selected spots (Figure 2c), gave rise to the image with parallel arrays of striations whose spacing was specified as above (Figure 2d). A set of reflections whose spacing was virtually identical to those above appeared also in the corresponding structure in chemically fixed Purkinje dendrites (data not shown). Takei *et al.* (1994) examined, by electron microscopy, cultured cells in which various constructs of mutant IP_3R molecules were overexpressed. What they found on the surface of the inclusion body were extensive rectangular arrays of intramembranous particles whose averaged spacing was 16.4 nm. Since the size of the structural unit they measured in their electron micrograph was very close to the value we found here, we checked if the molecular arrangement of IP_3R indicated in their figures had any features similar to ours. The Fourier spectrum obtained from a digitized image of their figure (inset of Figure 5 of Takei *et al.*, 1994, which is reproduced here in Figure 2e) showed two pairs of clear reflection spots (Figure 2f and g), the ratio of whose spacing was ~7:8 and not 1:1 as originally assumed. It is also notable that the angle between the lines connecting each pair of spots is not a right angle but is inclined by ~10°. Such a characteristic feature of the array was almost identical to ours, strongly suggesting that the component of the regular array we found in the stacked cisternae of bovine Purkinje cell would be IP_3R.

Structure and arrangement of receptor molecules on the membrane surface

In order to study the details of the intradendritic structure covered with this array, we attempted to examine the surface profile of the organelles in the neurites by freeze-fracture deep-etch replication of the molecular layer of the cerebellum, where most of the thick neurites might be derived from Purkinje cells. Figure 3a shows the replica image of such a Purkinje dendrite which is characterized

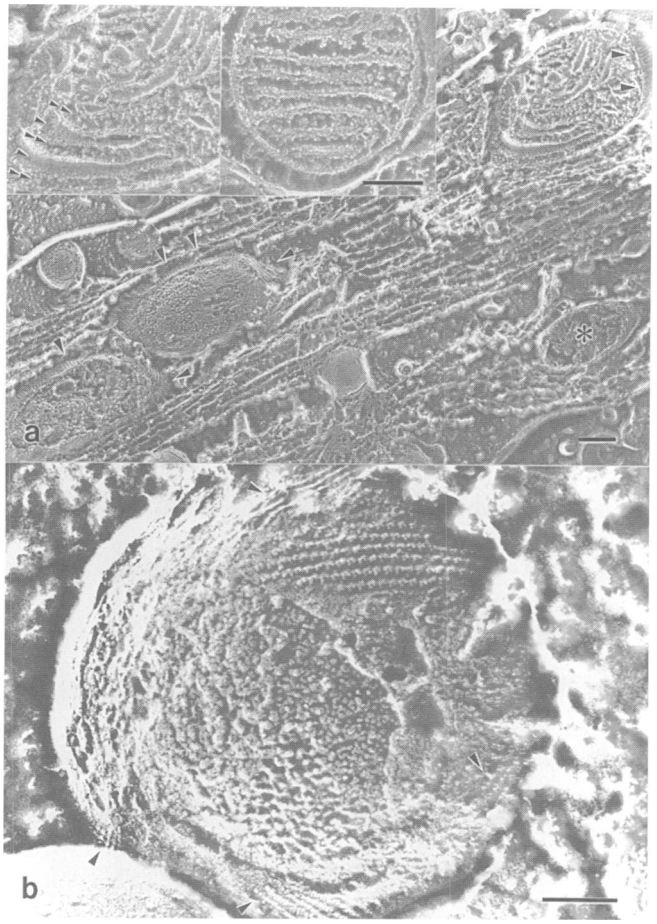

Fig. 3. (**a**) Electron micrograph of a quick-freeze deep-etch replica of a Purkinje cell dendrite. Two kinds of organelle are embedded among the parallel array of microtubules. The surfaces of large globular vesicles are covered with a parallel striation pattern (arrowheads). A mitochondrion is indicated by the asterisk. In the insets are the higher magnification views showing the characteristic alternating repeat of smooth (arrowhead) and rough (double arrowhead) textures of the inner membrane surfaces of the vesicular organelle in question (left) as compared with that of the intra-dendritic mitochondrion with a rough-surfaced inner membrane. Scale bars are 200 nm. (**b**) Closer view of the molecular lattice on the surface of a very deeply etched vesicle. Note that the oblique view of the same lattice gives a striation pattern (arrowheads) identical to those in (a). Scale bar is 100 nm.

by the presence of parallel arrays of microtubules and the globular membranous organelles in the space delineated by the cylindrical plasma membrane. On the true surface of many globular vesicles, we could often recognize the existence of a fine parallel striation pattern with regular spacing. This vesicular organelle was distinguished from mitochondria, all the surfaces of whose inner membrane were covered with numerous protrusions of F1-ATPase particles (right inset of Figure 3a) (Meller, 1983). It was identified as cisternal stacks by the characteristic feature of repeating alternate smooth and rough surfaces of the inner membrane (see high magnification view shown in the left inset of Figure 3a). Thus, the regular arrays commonly found in replicas and plastic-embedded sections strongly suggest the presence of some crystal-like structure on the membrane surface of cisternal stacks.

A further and more extensive search was made on replicas looking for fields where each molecule on the membrane might be resolved more clearly. Specimens with deeper etching than the standard protocol were useful for observing an face-on view of the receptor molecules in the neural cells, since the intraneuronal protein concentration is not so high that a large amount accumulates even under such conditions. Hence, the top portion of the vesicle with embedded receptors remained unperturbed by knife fracture, with the true surface being newly exposed by sublimation of the surrounding ice layer. Figure 3b indicates one of these fields in which many particles are arranged regularly in a two-dimensional crystalline lattice on the spherical surface of the vesicles, as described above. Though the apparent shape of individual particles differed minutely according to the orientation with respect to the shadowing source, each structural unit seemed to consist of a square-shaped particle with four equal sides measuring ~12 nm, suggesting a tetrameric structure. Using the computer program developed to measure the heights of specific points from the parallax values in the stereo images of the replica (kindly measured by Dr N.Baba, see the Appendix of Katayama *et al.*, 1996), we determined the inclination of the basal plane of the receptor particles and corrected a part of the image so that the plane of the centre of the field becomes normal to the line of vision (Figure 4a). Figure 4b indicates the Fourier spectrum from which the lattice points were extracted (Figure 4c) to give the filtered image (Figue 4d) after reverse transform, showing the face-on view of the lattice. The molecular arrangement is also demonstrated schematically in Figure 4e, where the elementary structural unit and the centres of rotational symmetry are exhibited. The centre–centre distance between structural units in each row (horizontal) was 14 nm, whereas it was 16 nm for those between neighbouring rows (oblique). Taking into account some extension of the plastic-embedded sections, which usually occurs upon irradiation by the electron beam, the agreement in the geometry of the molecular arrangement observed by two independent methodologies, freeze-substitution and freeze-etch replication, seems to be sufficiently good. The 4-fold symmetry of the structural unit was confirmed further by rotational correlation analysis of the particles (data not shown). It is notable that each square-shaped particle is arranged in such a way that one of its sides is inclined ~20° off from the row-line. The potential origin of such an arrangement is discussed below.

Comparison of the surface profile of the receptor with that of ryanodine receptor

Figure 5a shows three views selected from successively tilted micrographs taken at 20° apart, to give two stereo-paired images. In some of the particles which were optimally shadowed, the subunits appeared somewhat elongated to form a spiral shape like that of a ship's screw.

Since IP_3R is known to have homology to sRyaR in primary amino acid sequence together with its functions as Ca^{2+} channel, it is of great interest to compare their molecular architecture visualized by the same electron microscopy technique. Figure 5b shows a gallery of images of the sRyaR molecules visualized on the vesicles prepared from SR. The images not only showed the clear tetrameric nature of the total sRyaR moleclule *in situ*, but also revealed details on the surface of the subunit, indicating the superior spatial resolution of our freeze-fracture deep-etch replica technique over conventional shadowing after

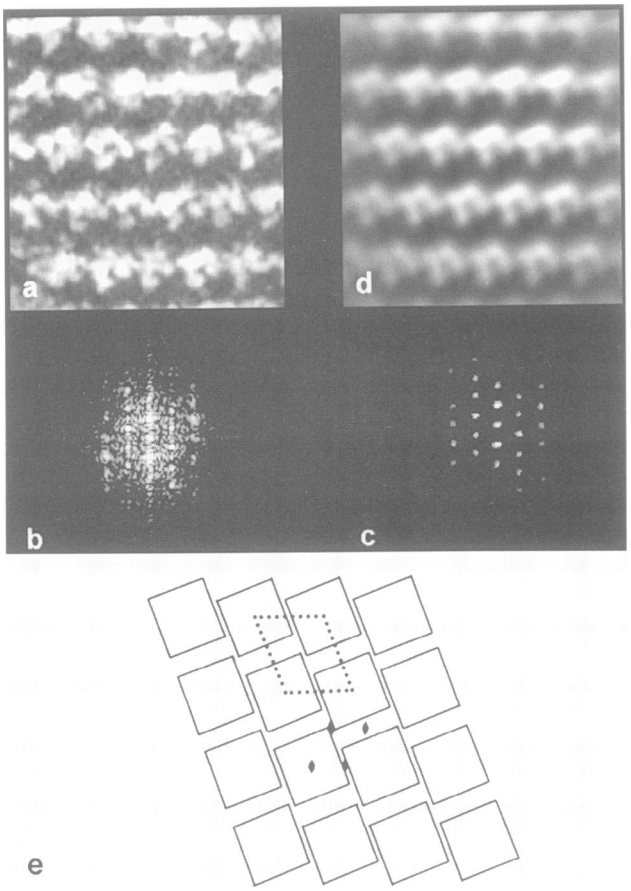

Fig. 4. (**a**) Arrays of receptor molecules whose distortion by the oblique view was corrected so that the membrane surface becomes almost normal to the line of vision. (**b**) Fourier spectrum of the field indicated in (a). (**c**) Selected spots used in the reverse transform. The distribution of reflection spots extends close to the 5 nm resolution limit. (**d**) Filtered image of (c). The molecular arrangement in the lattice and the tetrameric nature of each structural unit are evident. (**e**) Schematic diagram depicting the geometric arrangement of the molecules in the lattice. The dotted parallelogram indicates the elementary structural unit with the location of 2-fold rotation axes shown by pointed ellipses. The unit cell measures 14 nm (horizontal) and 16 nm (oblique), respectively. The ratio of these lengths is the same as found in the IP_3R-overexpressing COS cell.

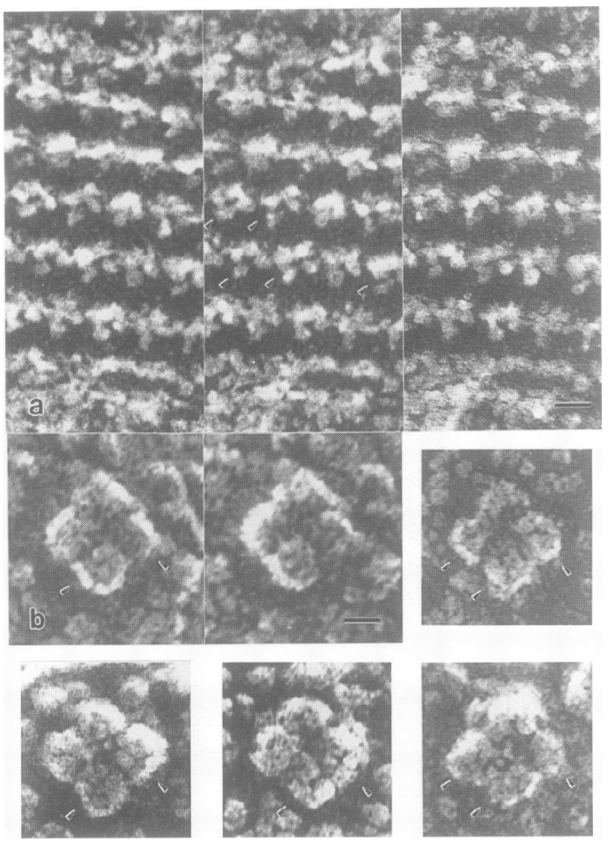

Fig. 5. (**a**) Triple tilted views of IP_3R to give two pairs of stereo images. Each image was taken at 20° from its neighbour. Note the optimally shadowed particles which look elongated and have a spiral shape (arrowheads). (**b**) One stereo pair and three assorted images of RyaR molecules on SR vesicles. Images were taken using the same method as for IP_3R, except for the use of mica flakes as the supporting material. Note the clear tetrameric structure and the crossed grooves on the surface of some of the subunits (arrowheads). The size of the total molecular assembly is almost twice that of IP_3R. Scale bars represent 10 nm. See text for details.

freeze-drying. The crossed grooves observed on the subunit of many particles are actually one of the main features of the three-dimensional structure averaged and reconstructed from frozen-hydrated cryo-electron microscopic images (Radermacher *et al.*, 1994).

The great surprise from this comparison was the size of the IP_3R, which was very small compared with sRyaR. The apparent size of IP_3R was close to half that of sRyaR, which implies that the shadowed surface area of the total IP_3R molecule approaches that of a single subunit of the tetrameric sRyaR, though otherwise they resembled each other in terms of tetrameric nature and the mode of disposition in the membrane plane.

Discussion

The dimensions of bovine Purkinje cells, as compared with those of the mouse (compare Figure 1a with the inset) or rat, were very large in terms of both length and diameter, both for the cell body and the dendrites. Bovine tissues could thus potentially be a good source for preparing large amounts of receptor proteins of neuronal type.

Though there have been various arguments regarding the actual existence and physiological function of cisternal stacks in Purkinje cells (Herndon, 1964; Karlsson and Schultz, 1966; Hansson, 1981), it seems a concrete fact that some factors such as anoxia would induce a variable amount of rearrangement of sER, leading to the production of membrane stacks presumably as one of the adaptive processes of the cell (Takei *et al.*, 1994). In fact, it was shown that the transformation of sER into cisternal stacks occurs quite rapidly after starting buffer perfusion of an animal, probably because of anoxaemic states (Takei *et al.*, 1994). We confirmed that such drastic transformation of mouse Purkinje cells starts within several minutes after sacrifice. Considering the time necessary to transport the bovine cerebellar material to the laboratory, it is naturally postulated that Purkinje cells would contain a large number of cisternal stacks which are very rich in IP_3R molecules on their membrane surface. Accordingly, we searched for the organelles with specialized membranous structure and actually found numerous vesicles with a regular striation pattern on their true surface. Further, the characteristic arrangement of the particles agreed very well with that found in cultured cells which had been converted to

overproduce IP_3R molecules. Thus, it seems highly likely that the particles which cover the vesicle surface represent IP_3R molecules.

We considered RyaR and the vesicular Ca^{2+}-ATPase pump (Ellisman *et al.*, 1991; Kuwajima *et al.*, 1992) as candidates for the constituent of such a two-dimensional crystalline lattice. Both of them have the ability, in some cases, to form a two-dimensional array on the membrane surface. Several immunochemical studies of cerebellar Purkinje cells indicate the co-existence of RyaR and IP_3R on sER, though the density of RyaR seems much less (Walton *et al.*, 1991; Kuwajima *et al.*, 1992). However, the shadowed surface profile of the sRyaR molecule prepared from SR was distinguished unambiguously from the structural element observed in the dendrites of Purkinje cells. It is known that Ca^{2+}-ATPase in scallop SR exists, *in situ*, in the form of a two-dimensional helical array on the surface of cylindrical vesicles (Castellani and Hardwicke, 1983). In mammalian muscle, addition of ATP/inorganic vanadate to SR vesicles induces analogous regular arrays of ATPase molecules as well (Dux and Martonosi, 1983), though the original arrangement of Ca^{2+}-ATPase molecule is not so regular. Despite the presence of a substantial amount of Ca^{2+}-ATPase in Purkinje cells, we did not observe any ordered array in an ATP/vanadate-treated microsome fraction. According to previous studies (Villa *et al.*, 1991; Takei *et al.*, 1992), the distribution of the immunochemical signal for Ca^{2+}-ATPase in the cerebellum is sparse and weak, existing only limitedly on the cytoplasmic surface of cisternal stacks. However, detailed analysis of such a crystalline structure in SR revealed that the lattice, whether naturally existing or artificially induced, consists of parallel rows of a dimeric structural element (Castellani *et al.*, 1985; Taylor *et al.*, 1986; Toyoshima *et al.*, 1993). Hence, the Ca^{2+}-ATPase molecule is not likely to be the constituent of the crystalline array found in Purkinje cells, in which the structural element is clearly tetrameric. All the experimental evidence above supports our conclusion that the particles making up the crystalline array can be identified as IP_3R in its native state, even though the cell might be in a pathological condition.

The most unexpected feature in the observed image of IP_3R was its very small size as compared with RyaR when visualized by the same technique. Though the negatively stained images of IP_3R isolated from cerebellum (Maeda *et al.*, 1991b) or smooth muscle (Chadwick *et al.*, 1990) were reported to have similar dimensions (20–25 nm) to RyaR, the difference in both the size and the shape of individual particles appeared to be very large, due to distortion, especially the flattening of the molecules that necessarily accompanies the staining procedure, or the binding of a variable amount of detergent micelles used to solubilize the proteins. As a simple geometrical relationships, the diameter of a globular particle should be proportional to the cube root of the particle's mass, if a constant mass/volume ratio is assumed. If such a straightforward calculation is applied to the case of these receptor molecules (e.g. 2749 amino acid residues for mouse IP_3R type 1 and 5037 residues for rabbit skeletal type RyaR), the expected diameter or the side length of the IP_3R should be as much as 80% of that of RyaR. According to the three-dimensional image reconstructed by Radermacher *et al.* (1994), the RyaR molecule is characterized by a loosely packed assembly with >50% of the enveloped volume occupied by water, presumably an adaptation to its function in a specially differentiated environment; the top of the tetrameric molecule might be covered by the dihydropyridine receptor and still the channel must allow the flow of massive amounts of Ca^{2+} in a very short time. The authors discussed that the volume estimated by electron microscopy would be two to three times greater than that expected from its molecular weight. If a 3-fold excess volume is assumed, then the estimated ratio of the molecular dimension of IP_3R to sRyaR would be 56%, which might reasonably agree with the actual observation. Further, the estimated size of overexpressed IP_3R in COS cells (Takei *et al.*, 1994) or in *Sf9* cells infected by baculovirus vector (our unpublished data) was very close to the present results, providing strong support for our view that the size of IP_3R is quite small. Thus, all the data and arguments are compatible with our identification of the particles in the regular array as IP_3R molecules. As a corollary, we may predict that the intramolecular folding of IP_3R molecules would not be so loose as in RyaR, and the central hole or pit visualized in our replica could be a good candidate for the channel that gives a specific permeability to Ca^{2+}. This also might partly account for the experimental finding that the conductance of an IP_3-gated channel (Ehrich and Watras, 1988; Maeda *et al.*, 1991a; Watras *et al.*, 1991) is much smaller than that through a caffeine-gated RyaR channel (Ehrich and Watras, 1988), though the final values may be greatly influenced by many other factors.

The angled position of the square-shaped elements in the molecular lattice is of some interest. Though the origin of such an arrangement might be explained in various ways, one possibility is the localization of strongly charged groups of the same polarity on the outside of the subunits which would oppose each other if the square-shape was placed side-by-side without an intervening space. The spaces between structural elements might be determined by the balance of repulsive force which may operate between those charges (see Katayama and Nonomura, 1979) and the surface tension to pack the molecules as tightly as possible in a limited area. The presence of a similar kind of disposition has been reported in two-dimensional crystalline arrays of other homotetrameric particles such as RyaR on junctional SR (Loesser *et al.*, 1992) or membrane-bound ribosomes of the egg crystallized under low temperature conditions (Unwin, 1977; Heuser, 1983), though the actual molecular arrangements or the intermolecular forces which operate for the arrangement might differ in each case.

The formation of cisternal stacks may work potentially as a protective process of Purkinje cells in anoxaemic conditions. In these conditions, most IP_3R molecules seem to oppose each other head-to-head, as if they block each other with the top portion of the molecules, superficially in a manner similar to gap junctions. IP_3R itself could have the property of self-associating under some pathological conditions. Such a configuration could be advantageous to prevent the leakage of Ca^{2+} from its storage compartment when the Ca^{2+}-ATPase pump eventually ceases to sequester cytoplasmic Ca^{2+} under anoxaemic conditions. Alternatively, the association of opposing molecules

belonging to different cisternae might form a large Ca^{2+} storage pool which could be another compensatory reaction to anoxia. On the other hand, there is another view that cisternal stacks by themselves might not work as an efficient compartment for Ca^{2+} storage, since they lack low affinity, high capacity Ca^{2+} binding proteins whose presence in the lumenal space characterizes the functional Ca^{2+}-accumulating compartment (Villa *et al.*, 1991; Takei *et al.*, 1992). In crucial neurons such as Purkinje cells, IP_3R would operate to delicately control the local Ca^{2+} concentration of individual segments separately. Since the permeability of each IP_3R is much smaller than that of RyaR, cells may need a continuous supply of numerous IP_3R molecules which might be transported from the cell body to each location as required. There must be an abundant reservoir to store and supply a large number of IP_3R molecules, particularly for very long dendrites. Thus, the giant Purkinje cells in bovine cerebellum might require especially large stocks of IP_3R, which are accumulated constantly in the most efficient and space-saving form, the two-dimensional crystals. We observed a similar molecular array in porcine Purkinje neurons (our unpublished data) which are also large cells.

In order to understand the functions of IP_3R from a structural aspect, it is obviously necessary to investigate various ligand binding sites and the structural change caused by the ligands, from a three-dimensional viewpoint. Studies are in progress to examine if any conformational difference is observed when the receptor receives the signal from IP_3, its natural ligand, or adenophostin, a newly developed agonist (Hirota *et al.*, 1995).

Materials and methods

Materials

We used bovine cerebellum as a suitable material for electron microscopy, because of its very large dimensions both in terms of cell body and proximal dendritic trunk. Bovine cerebellum was obtained from a local slaughterhouse and transported to the laboratory in ice. The tissue was sliced sagitally into sections of ~1 mm thickness and kept briefly in buffer solution [20 mM HEPES, 150 mM NaCl, 2 mM $MgCl_2$, 1 mM EGTA, 1 mM phenylmethylsulfonyl fluoride, 21 μM leupeptin, 10 μM *trans*-epoxysuccinyl-L-leucylamido(4-guanidino)butane (E-64), pH 7.0] at room temperature. The molecular layers of the slices were trimmed out and mounted onto a slab of fixed lung or directly onto an aluminium disk for quick-freezing.

Rabbit SR vesicles enriched with RyaR were prepared as the heavy microsomal fraction, according to Meissner *et al.* (1986).

Polyclonal antibody against IP_3R was raised in rabbits by repeated injection of mouse receptor which was purified according to Nakade *et al.* (1994). The IgG fraction was prepared and purified by a conventional method on a column of immobilized protein A.

Conventional immunofluorescence microscopy with frozen sections

Sagital slices from mouse or bovine cerebellar tissues were fixed at 4°C for 1 h with 4% formaldehyde in 0.1 M phosphate buffer. After impregnation in sucrose, specimens were sectioned and subjected to immunofluorescent staining.

Qiuck-freezing for electron microscopy

Tissue samples were frozen quickly by contact onto a pure copper block (Polaron E-7200) cooled to liquid helium temperature (Heuser *et al.*, 1979). Frozen samples were stored in liquid nitrogen until further processing. Solution samples such as SR vesicles were adsorbed to mica flakes (Heuser, 1983; Katayama, 1989) before freezing, followed by the same procedure. Mica flakes were very effective as a spacer material to keep low viscosity samples in a solid form.

Freeze substitution and immunocytochemical detection

A part of the quick-frozen samples was freeze-substituted at −80°C for 2 days in acetone containing 2% tannic acid as a fixative. Then they were transferred to higher temperature according to a standard protocol (Usukura, 1993) and embedded in LR-White resin. Thin sections were made and picked up on a nickel grid for immunodetection. After blocking with normal goat serum, sections were incubated with primary antibody followed by secondary antibody with 10 nm colloidal gold probes, with extensive washing steps intervening. Semithin sections (1.0 μm) from the same sample were stained with fluorescent secondary antibody, to examine the detailed distribution of the organelles in a wide field, as probed by antibody. Since the fluorecent signal was too weak for conventional photography, a cooled-CCD camera (SBIG ST-8, Magellan Co., Kyoto, Japan) was used for effectively imaging such specimens.

Freeze-fracture deep-etching and replication

Quick-frozen cerebellar tissues were subjected to deep-etch replication by a standard protocol (Katayama, 1989) with a Balzers-300 freeze-etch unit. In brief, after maintaining the temperature at −120°C for 15 min, the temperature of the stage was raised to −104°C and left to stand for 5 min. Then the samples were knife fractured and usually etched for 4 min, covered with a cold knife as a vapour trap, followed by rotary shadowing with Pt/C (20° elevation angle) and backing with carbon. Etching time was prolonged to 6–8 min when needed. After dissolving the tissue with household bleach, specimens were rinsed with water three times and picked up onto a hexagonal copper grid for examination in a JEM-2000ES transmission electron microscope (JEOL). Solution samples adsorbed on mica flakes were treated in a similar manner except for the use of full-strength hydrofluoric acid for mica dissolution.

Electron microscopic examination and subsequent image processing

Electron micrographs of replica specimens were usually taken as stereo-pairs with ± 10° tilt angles. Some of the electron micrographs were further subjected to image analyses by a computer. Images were digitized (1000 dpi; 1.7 nm/pixel) by a film scanner, and the Fourier spectra were taken using a Luzex-F real-time image analyser (Nireco, Japan) linked to a personal computer. After checking the significant and strong peaks from the spectra, the selected signals were passed for reverse transform to give filtered images of the molecular array. In order to obtain the face-on view of the receptor arrays on the globular vesicle surface in replica images, the averaged inclination angle of the plane of the selected area was measured by stereo-photogrammetry (Katayama *et al.*, 1996) and the distortion was corrected by commercial mapping software.

Acknowledgements

We are especially grateful to Dr P.De Camilli for generous permission to use Figure 5 of Takei *et al.* (1994) for our Fourier analysis, described in Figure 2 of our paper. We are greatly indebted also to Dr J.M.Murray for his critical reading of the manuscript with constructive suggestions and to Dr J.E.Heuser for his comments. This work was supported by a Grant-in-Aid for Scientific Research, a Grant-in-Aid for the Research of Priority Areas and a Grant-in-Aid for Developmental Scientific Research to E.K., and partly by a Grant-in-Aid for Specially Promoted Research to K.M. from the Ministry of Education, Science, Sports and Culture of Japan.

References

Block,B.A., Imagawa,T., Campbell,K.P. and Franzini-Armstrong,C. (1988) Structural evidence for direct interaction between the molecular components of the transverse tubule/sarcoplasmic reticulum junction in skeletal muscle. *J. Cell Biol.*, **107**, 2587–2600.

Castellani,L. and Hardwicke,M.D. (1983) Crystalline structure of sarcoplasmic reticulum from scallop. *J. Cell Biol.*, **97**, 557–561.

Castellani,L., Hardwicke,M.D. and Vibert,P. (1985) Dimer ribbons in the three-dimensional structure of sarcoplasmic reticulum. *J. Mol. Biol.*, **185**, 579–594.

Chadwick,C., Saito,A. and Fleischer,S. (1990) Isolation and characterization of the inositol trisphosphate receptor from smooth muscle. *Proc. Natl Acad. Sci. USA*, **87**, 2132–2136.

Dux,L. and Martonosi,A. (1983) Two-dimensional arrays of proteins in sarcoplasmic reticulum and purified Ca^{2+}-ATPase vesicles treated with vanadate. *J. Biol. Chem.*, **258**, 2599–2603.

Ehrlich,B.E. and Watras,J. (1988) Inositol 1,4,5-trisphosphate activates a channel from smooth muscle sarcoplasmic reticulum. *Nature*, **336**, 583–586.

Ellisman,M.H., Deerinck,T.J., Ouyang,Y., Beck,C.F., Tansley,S.J., Walton,P.D., Airey,J.A. and Sutko,J.L. (1991) Identification and localization of ryanodine binding proteins in the avian central nervous system. *Neuron*, **5**, 135–146.

Ferris,C.D., Huganir,R.L., Supattapone,S. and Snyder,S.H. (1989) Purified inositol 1,4,5-trisphosphate receptor mediates calcium flux in reconstituted lipid vesicles. *Nature*, **342**, 87–89.

Franzini-Armstrong,C. (1970) Studies of the triad. I. Structure of the junction in frog twitch fibers. *J. Cell Biol.*, **47**, 488–499.

Franzini-Armstrong,C. and Nunzi,G. (1983) Junctional feet and particles in the triads of fast twitch muscle fibers. *J. Muscle Res. Cell Motil.*, **4**, 233–252.

Furuichi,T., Yoshikawa,S., Miyawaki,A., Wada,K., Maeda,N. and Mikoshiba,K. (1989) Primary structure and functional expression of the inositol 1,4,5-trisphosphate binding protein P400. *Nature*, **342**, 32–38.

Furuichi,T., Kohda,K., Miyawaki,A. and Mikoshiba,K. (1994) Intracellular channels. *Curr. Opin. Neurobiol.*, **4**, 294–303.

Hansson,H.A. (1981) Lamellar bodies in Purkinje nerve cells experimentally induced by electric field. *Brain Res.*, **216**, 187–191.

Herndon,R. (1964) Lamellar bodies, an unusual arrangement of the granular endoplasmic reticulum. *J. Cell Biol.*, **20**, 338–342.

Heuser,J.E. (1981) Quick-freeze deep-etch preparation of samples for 3-D electron microscopy. *Trends Biochem. Sci.*, **6**, 64–68.

Heuser,J.E. (1983) Procedure of freeze-drying molecules adsorbed to mica flakes. *J. Mol. Biol.*, **169**, 155–195.

Heuser,J.E. (1989) Protocol for 3-D visualization of molecules on mica via the quick-freeze deep-etch technique. *J. Electron Microsc. Techniques*, **13**, 244–263.

Heuser,J.E., Reese,T.S., Jan,L.Y., Jan,Y.N., Dennis,M.J. and Evans,L. (1979) Synaptic vesicle exocytosis captured and correlated with quantal transmitter release. *J. Cell Biol.*, **81**, 275–300.

Hirota,J., Michikawa,T., Miyawaki,A., Takahashi,M., Tanzawa,K., Okura,I., Furuichi,T. and Mikoshiba,K. (1995) Adenophostin-mediated quantal Ca^{2+} release in the purified and reconstituted inositol 1,4,5-trisphosphate receptor type I. *FEBS Lett.*, **368**, 248–252.

Karlsson,U. and Schultz,R.L. (1966) Fixation of the central nervous system for electron microscopy by aldehyde perfusion. III. Structural changes after exanguination and delayed perfusion. *J. Ultrastruct. Res.*, **14**, 47–63.

Katayama,E. (1989) The effect of various nucleotides on the structure of actin-attached myosin subfragment-1 studied by quick-freeze deep-etch electron microscopy. *J. Biochem.*, **106**, 751–770.

Katayama,E. and Nonomura,Y. (1979) Electron microscopic analysis of tropomyosin paracrystals. *J. Biochem.*, **86**, 1511–1522.

Katayama,E., Shiraishi,T., Oosawa,K., Baba,N. and Aizawa,S.-I. (1996) Geometry of the flagellar motor in the cytoplasmic membrane of *Salmonella typhimurium* as determined by stereo-photogrammetry of quick-freeze deep-etch replica images. *J. Mol. Biol.*, **255**, 458–475.

Kuwajima,G., Futatsugi,A., Niinobe,M., Nakanishi,S. and Mikoshiba,K. (1992) Two types of ryanodine receptors in mouse brain: skeletal muscle type exclusively in Purkinje cells and cardiac muscle type in various neurons. *Neuron*, **9**, 1133–1142.

Loesser,K., Castellani,L. and Franzini-Armstrong,C. (1992) Dispositions of junctional feet in muscles of invertebrates. *J. Muscle Res. Cell Motil.*, **13**, 161–173.

Maeda,N., Kawasaki,T., Nakade,S., Yokota,N., Taguchi,T., Kasai,M. and Mikoshiba,K. (1991a) Structural and functional characterization of inositol 1,4,5-trisphosphate receptor channel from mouse cerebellum. *J. Biol. Chem.*, **266**, 1109–1116.

Maeda,N., Niinobe,M. and Mikoshiba,K. (1991b) A cerebellar Purkinje cell marker P400 protein is an inositol 1,4,5-trisphosphate ($InsP_3$) receptor protein. Purification and characterization of $InsP_3$ receptor complex. *EMBO J.*, **9**, 61–67.

Meissner,G., Darling,E. and Eveleth,J. (1986) Kinetics of rapid Ca^{2+} release by sarcoplasmic reticulum: effects of Ca^{2+}, Mg^{2+} and adenine nucleotides. *Biochemistry*, **25**, 236–244.

Meller,K. (1983) Ultrastructural aspect of rapid-frozen, deep-etched and rotary-shadowed synaptosomes. *Cell Tissue Res.*, **231**, 347–355.

Mignery,G.A., Newton,C.L., Archer,B.T. and Südhof,T.C. (1990) Structure and expression of the rat inositol 1,4,5-trisphosphate receptor. *J. Biol. Chem.*, **265**, 12679–12685.

Mikoshiba,K., Furuichi,T. and Miyawaki,A. (1994) Structure and function of IP_3 receptors. *Semin. Cell Biol.*, **5**, 273–281.

Morris,E.P., Katayama,E. and Squire,J.M. (1994) Evaluation of high-resolution shadowing applied to freeze-fractured deep-etched particles: 3-D helical reconstruction of shadowed actin filaments. *J. Struct. Biol.*, **113**, 47–55.

Nakade,S., Rhee,S.K., Hamanaka,H. and Mikoshiba,K. (1994) Cyclic AMP-dependent phosphorylation of an immunoaffinity purified homotetrameric inositol 1,4,5-trisphosphate receptor (type 1) increases Ca^{2+} flux in reconstituted lipid vesicles. *J. Biol. Chem.*, **269**, 6735–6742.

Otsu,H., Yamamoto,A., Maeda,N., Mikoshiba,K. and Tashiro,Y. (1990) Immunogold localization of inositol 1,4,5-trisphosphate ($InsP_3$) receptor in mouse cerebellar Purkinje cells using three monoclonal antibodies. *Cell Struct. Funct.*, **15**, 163–173.

Pozzan,T., Rizzuto,R., Volpe,P. and Meldolesi,J. (1994) Molecular and cellular physiology of intracellular calcium stores. *Physiol. Rev.*, **74**, 595–636.

Radermacher,M., Rao,V., Grassucci,R., Frank,J., Timerman,P., Fleischer,S. and Wagenknecht,T. (1994) Cryo-electron microscopy and three-dimensional reconstruction of the calcium release channel/ryanodine receptor from skeletal muscle. *J. Cell Biol.*, **127**, 411–423.

Rusakov,D.A., Podini,P., Villa,A. and Meldolesi,J. (1993) Tridimensional organization of Purkinje neuron cisternal stacks, a specialized endoplasmic reticulum subcompartment rich in inositol 1,4,5-trisphosphate receptors. *J. Neurocytol.*, **22**, 273–282.

Saito,A., Inui,M., Radermacher,M., Frank,J. and Fleischer,S. (1988) Ultrastructure of calcium release channel of sarcoplasmic reticulum. *J. Cell Biol.*, **107**, 211–219.

Takei,K., Stukenbrok,H., Metcalf,A., Mignery,G.A., Südhof,T.C., Volpe,P. and De Camilli,P. (1992) Ca^{2+} stores in Purkinje neurons: endoplasmic reticulum subcompartments demonstrated by the heterogenous distribution of the $InsP_3$ receptor, Ca^{2+}-ATPase and calsequestrin. *J. Neurosci.*, **12**, 489–505.

Takei,K., Mignery,G.A., Mugnaini,E., Südhof,T.C. and De Camilli,P. (1994) Inositol 1,4,5-trisphosphate receptor causes formation of ER cisternal stacks in transfected fibroblasts and in cerebellar Purkinje cells. *Neuron*, **12**, 327–342.

Takeshima,H. *et al.* (1989) Primary structure and expression from complementary DNA of skeletal muscle ryanodine receptor. *Nature*, **339**, 439–444.

Taylor,K.A., Dux,L. and Martonosi,A. (1986) Three-dimensional reconstruction of negatively stained crystals of the Ca^{2+}-ATPase from muscle sarcoplasmic reticulum. *J. Mol. Biol.*, **187**, 417–427.

Toyoshima,C., Sasabe,H. and Stokes,D.L. (1993) Three-dimensional cryo-electron microscopy of the calcium ion pump in the sarcoplasmic reticulum membrane. *Nature*, **362**, 469–471.

Unwin,P.N.T. (1977) Three-dimensional model of membrane-bound ribosomes obtained by electron microscopy. *Nature*, **269**, 118–122.

Usukura,J. (1993) Rapid freezing and subsequent preparation methods in retinal cell biology. *Methods Neurosci.*, **13**, 37–53.

Van Nimvegen,D. and Sheldon,H. (1966) Early postmortem changes in cerebellar neurons of rat. *J. Ultrastruct. Res.*, **14**, 36–46.

Villa,A., Podini,P., Clegg,D.O., Pozzan,T. and Meldolesi,J. (1991) Intracellular Ca^{2+} stores in chicken Purkinje neurons: differential distribution of the low affinity–high capacity Ca^{2+} binding protein, calsequestrin, of Ca^{2+} ATPase and of the ER luminal protein Bip. *J. Cell Biol.*, **113**, 779–791.

Wagenknecht,T., Grassucci,R., Frank,J., Saito,A., Inui,M. and Fleischer,S. (1989) Three-dimensional architecture of the calcium/foot structure of sarcoplasmic reticulum. *Nature*, **338**, 167–170.

Walton,P.D., Airey,J.A., Sutko,J.L., Beck,C.F., Mignery,G.A., Südhof, T.C., Deerinck,T.J. and Ellisman,M.H. (1991) Ryanodine and inositol trisphosphate receptors coexist in avian cerebellar Purkinje neurons. *J. Cell Biol.*, **113**, 1145–1157.

Watras,J., Bezprozvanni,I. and Ehrlich,B.E. (1991) Inositol 1,4,5-trisphosphate-gated channels in cerebellum: presence of multiple conductance states. *J. Neurosci.*, **11**, 3239–3245.

Yamamoto,A., Otsu,H., Yoshimori,T., Maeda,N., Mikoshiba,K. and Tashiro,Y. (1991) Stacks of flattened smooth endoplasmic reticulum enriched in inositol 1,4,5-trisphosphate ($InsP_3$) receptor in mouse cerebellar Purkinje cells. *Cell Struct. Funct.*, **16**, 419–432.

Received on May 16, 1996; revised on June 10, 1996